Developments in the nonlinear capability of M3D-C^1

June 12,13

Madison, Wisc

N. Ferraro, S. Jardin, J. Chen
…. Primary developers

M. Shephard, Fan Zhang, …. (RPI SCOREC Center)
…. meshing, data layout, solver interface,…

J. Breslau, G. Fu, W. Park, H. Strauss, L. Sugiyama, …..
…. M3D team (likely future developers and users)

B. Lyons, J. Ramos
…. Kinetic effects

Also: PETSc Team (Hong Zhang), SuperLU Team (X. Li), …..

Goals of nonlinear M3D-C^1

- Long time simulations to cover ideal, reconnection, and transport timescales in same simulation
  - Do not start run from unphysical unstable state, let it evolve into one
  - Large S and wide separation of timescales enabled by large $\Delta t \sim$ 10-100 τ_A
  - Implies need for current controller, transport model, density and heat sources
- High resolution and convergence studies to obtain quantitative results
- Build physical model to be increasingly realistic 2F + kinetic model of plasma
- Concentrate on applications of relevance to ITER
  - Validation studies on existing experiments as available
- Strive to be community code with sufficient documentation for others to use and contribute to
  - Should be viewed as an resource (not as a threat)
- FY12: Demonstration runs with ~ 1000p
- FY13: Will apply for INCITE time for higher resolution runs with ~10,000p

outline

- Preconditioner effect on eigenvalues and condition number
- New time advance options
- Resistive MHD long-time runs with density and 2 temperatures
  - Stationary helical state
  - Sawtoothing discharge
- 2-fluid algorithm
  - Ion velocity form for velocity preconditioner
  - Harned-Mikic terms
  - Testing in 2D
  - Testing in 3D

M3D-C^1 can be run with 1, 2, or 3 velocity variables. Tracking the eigen-values shows how they separate into 3 groups (before preconditioning)

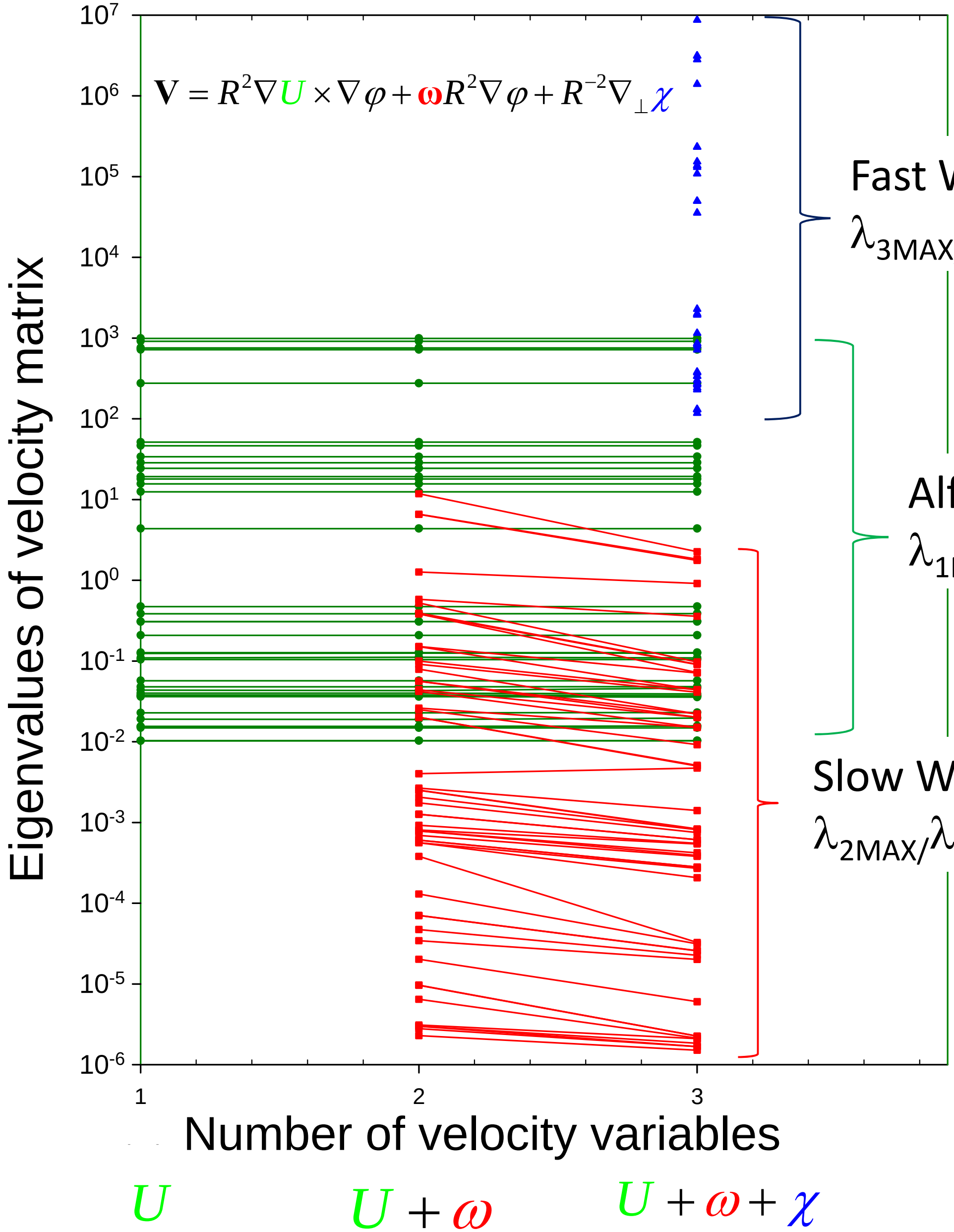

Fast Wave

$\lambda_{3MAX}/\lambda_{3MIN}$ =7.3 E4

Alfven Wave

$\lambda_{1MAX}/\lambda_{1MIN}$ =9.9 E4

Slow Wave

$\lambda_{2MAX}/\lambda_{2MIN}$ =1.46 E6

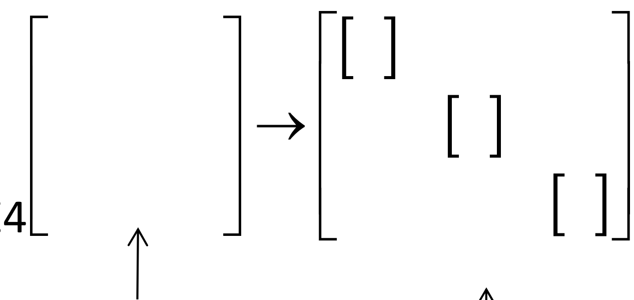

Original matrix:
$\lambda_{MAX}/\lambda_{MIN} = 10^{13}$

Annihilation operators split this into 3 loosely connected matrices, each with a condition number much less than original matrix

$$\lambda_1 = \left(\rho_0 + s k_\parallel^2 B_0^2\right) k_\perp^2$$

$$\lambda_2 \cong \left(\rho_0 + s k_\parallel^2 \gamma p_0\right)$$

$$\lambda_3 \cong -k_\perp^2 \left(\rho_0 + s k^2 B_0^2 + s k_\perp^2 \gamma p_0\right)$$

Velocity matrix is then preconditioned with a block-Jacobi preconditioner, which corresponds to a direct solve of all 2D “in plane” submatrices

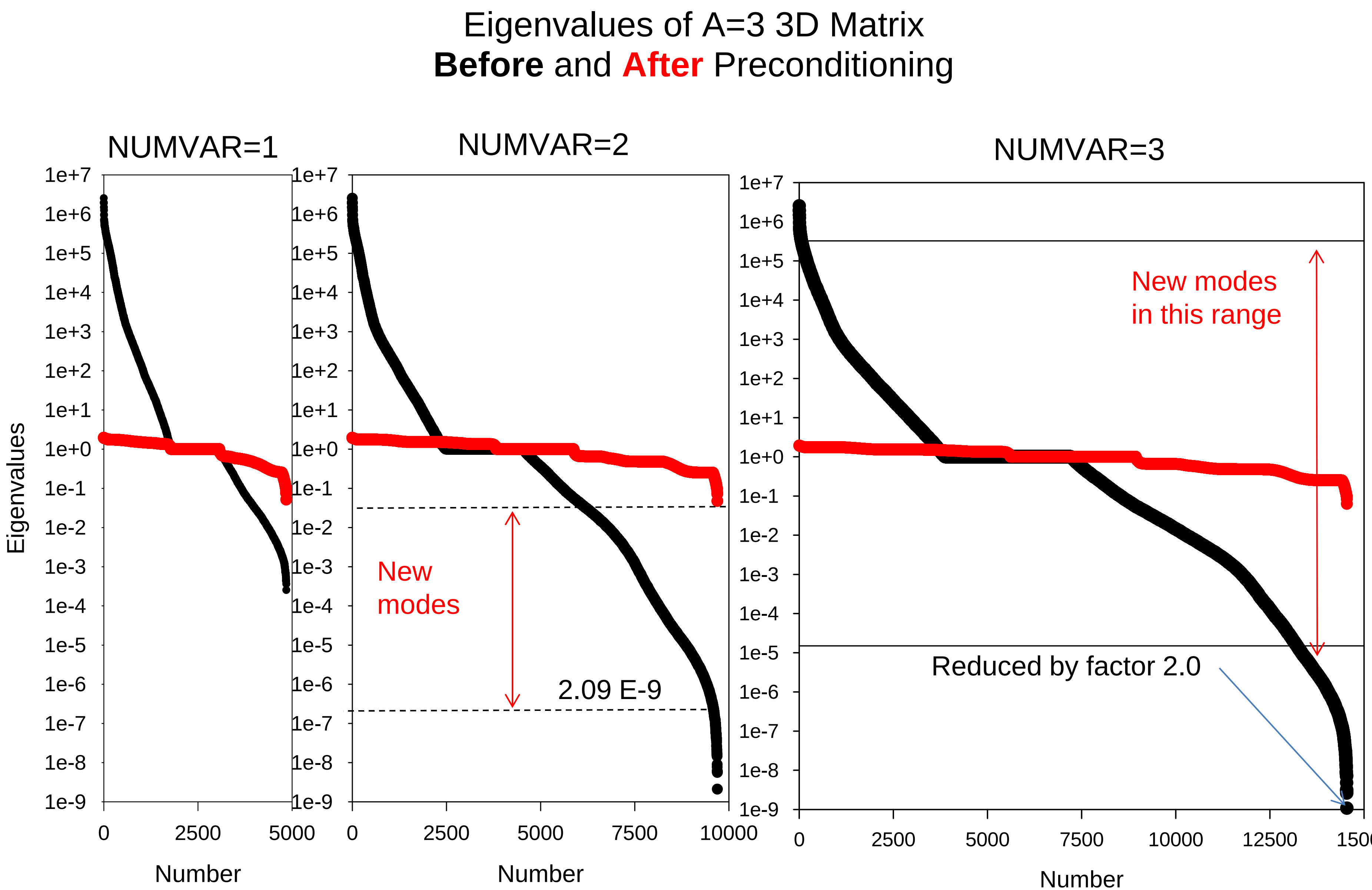

Some Conclusions and observations

- Condition number of preconditioned matrix is good (~ 30)!!
- However, condition number of linear matrices (before preconditioning) is large
  - 10^{16} (A=10) -- 10^{17} (A=3)
- May be able to improve condition number by shifting the eigenvalues associated with the variable ω up so they coincide with the others.
  - These are the new eigenvalues that appear when NUMVAR=2
- Can this be done by just renormalizing the field ω ??
  - However, ot clear that the condition number of entire matrix is important since the three blocks are approximately uncoupled

New time advance options

$$\mathbf{V} = R^2 \nabla U \times \nabla \varphi + \boldsymbol{\omega} R^2 \nabla \varphi + R^{-2} \nabla_\perp \chi$$

$$\mathbf{B} = \nabla \psi \times \nabla \varphi - \nabla_\perp f' + F \nabla \varphi : \qquad \nabla_\perp^2 f = F - F_0$$

$$p_e = nT_e \quad \& \quad p_i = nT_i$$

Old split advance

$$\begin{bmatrix} U \\ \omega \\ \chi \end{bmatrix}^{n+1} \rightarrow \begin{bmatrix} \psi \\ F \\ p_e \end{bmatrix}^{n+1} + \begin{bmatrix} p_i \end{bmatrix}^{n+1} + \begin{bmatrix} n \end{bmatrix}^{n+1}$$

New split advance

$$\begin{bmatrix} U \\ \omega \\ \chi \end{bmatrix}^{n+1} \rightarrow \begin{bmatrix} \psi \\ F \end{bmatrix}^{n+1} + \begin{bmatrix} T_e \\ T_i \end{bmatrix}^{n+1} + \begin{bmatrix} n \end{bmatrix}^{n+1}$$

Advantages:

- Advancing temperatures rather than pressure is necessary for stable implicit advance when the (large) parallel thermal conductivity is included

- Advancing the two temps. together allows implicit treatment of equi-partition term

Application: Can we explain the differences in sawtooth behavior for bean-shaped and elliptical-shaped plasmas that has been well documented experimentally (Lazarus, Tobias, …)

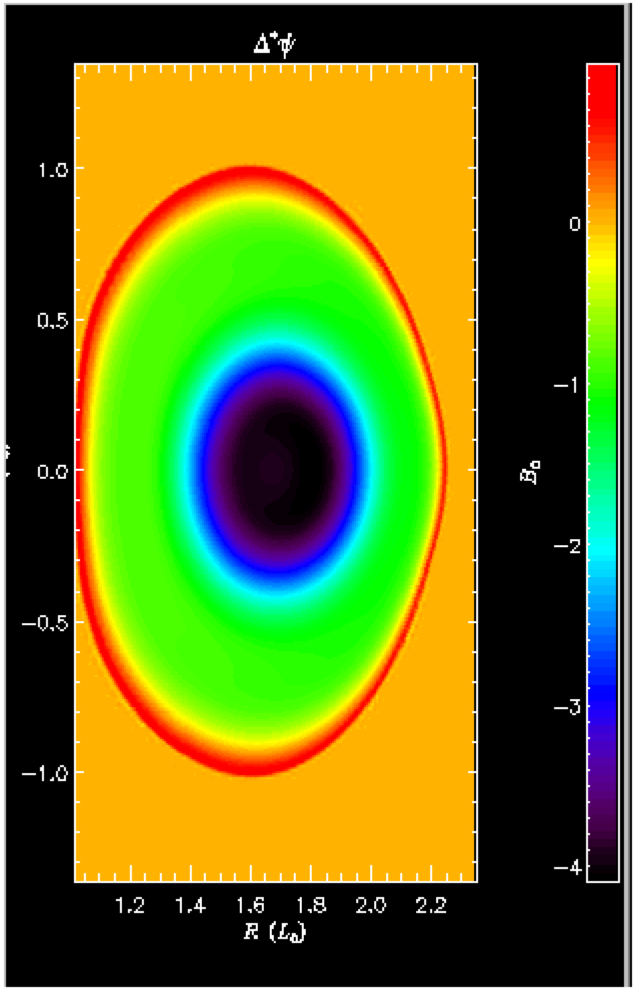

DIII-D shot 118164

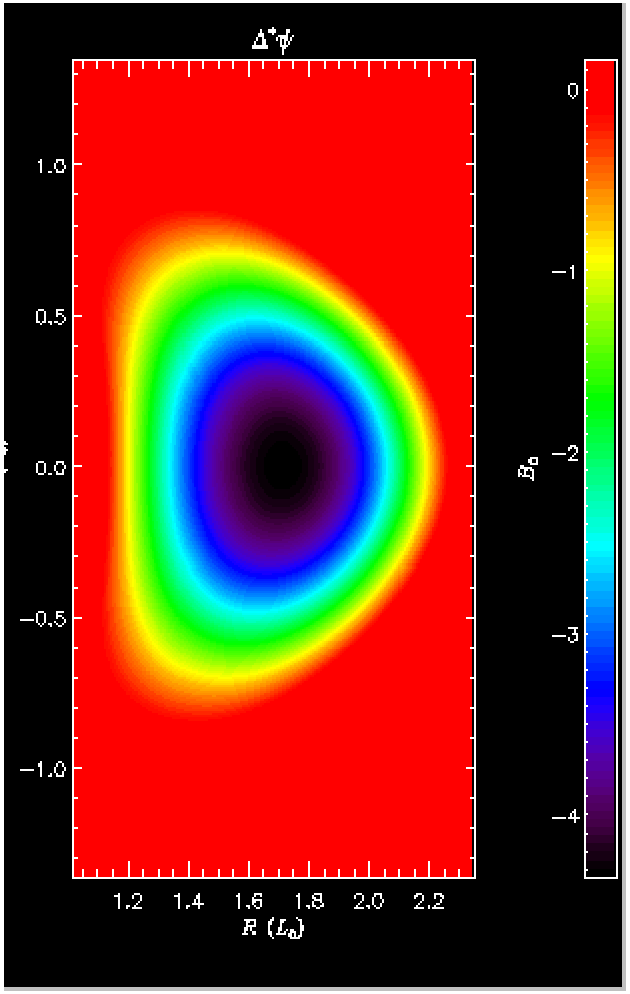

DIII-D shot 118162

We have imported these equilibria from geqdsk files, and inferred the transport properties from the plasma properties…simulations in progress

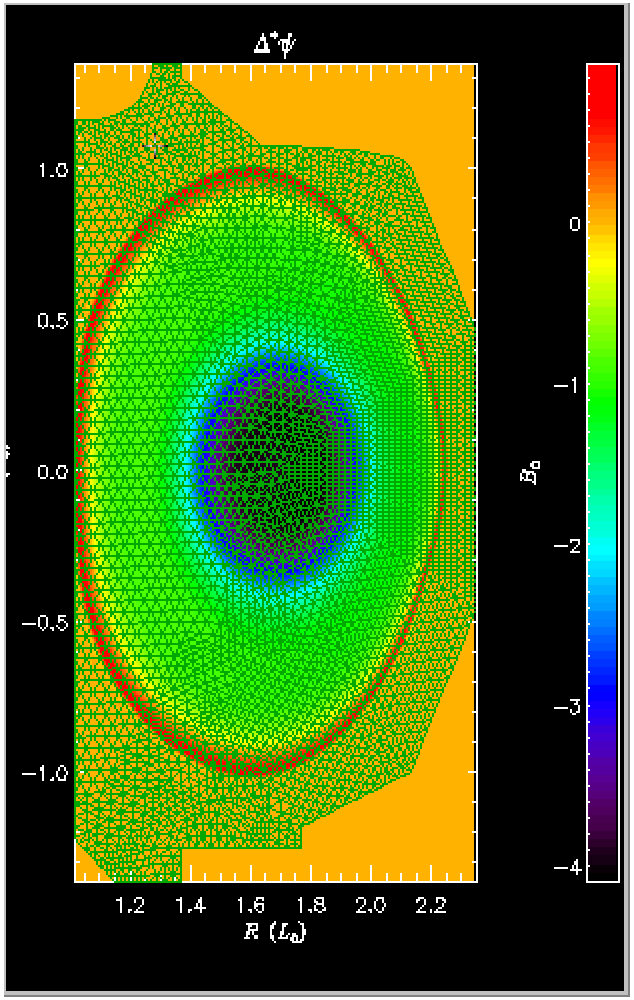

DIII-D shot 118164

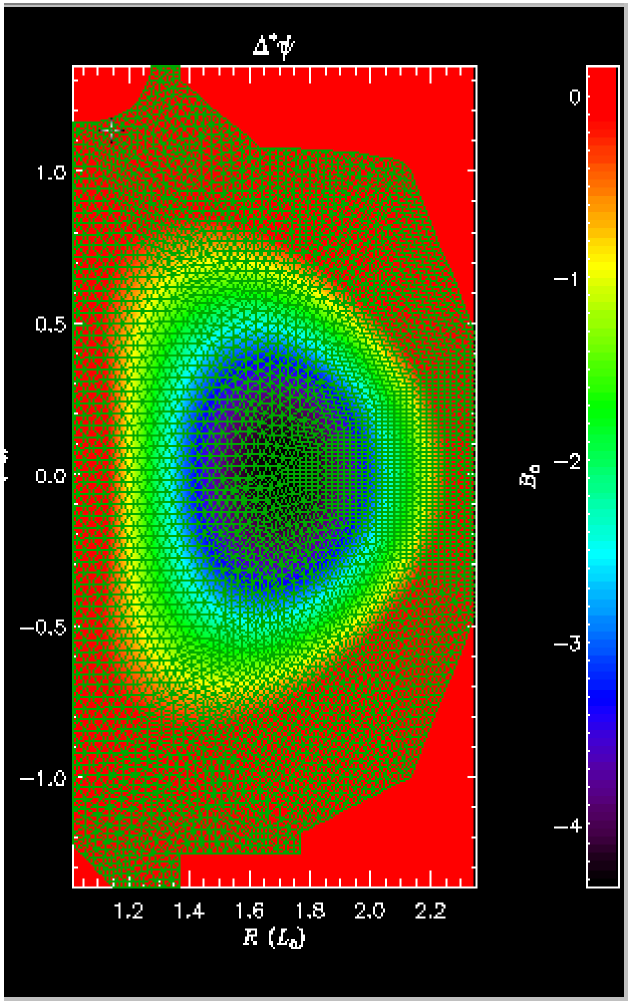

DIII-D shot 118162

Goal is to match MHD spectra and 2D ECEI data from Tobias, et al.

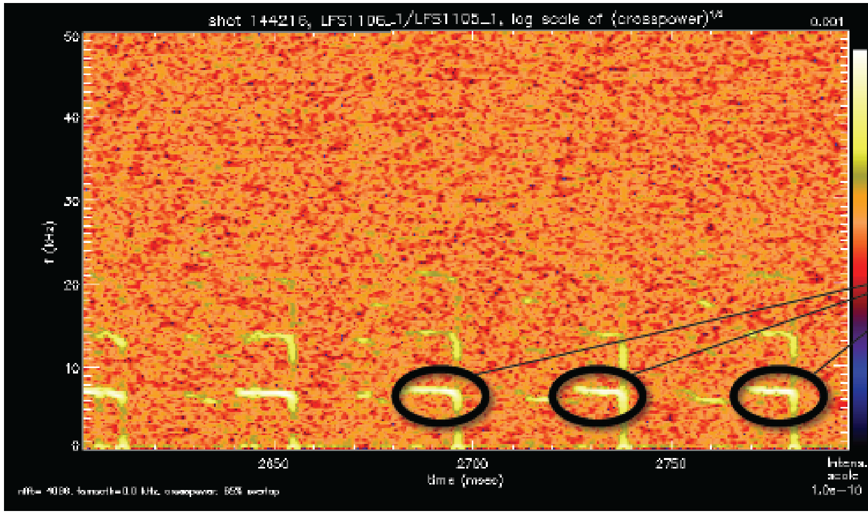

Sustained, saturated m/n=1/1 mode precedes crash

At or above core rotation estimate from CERQUICK

Oval (shots 144215, 16, 17, 19, 20)

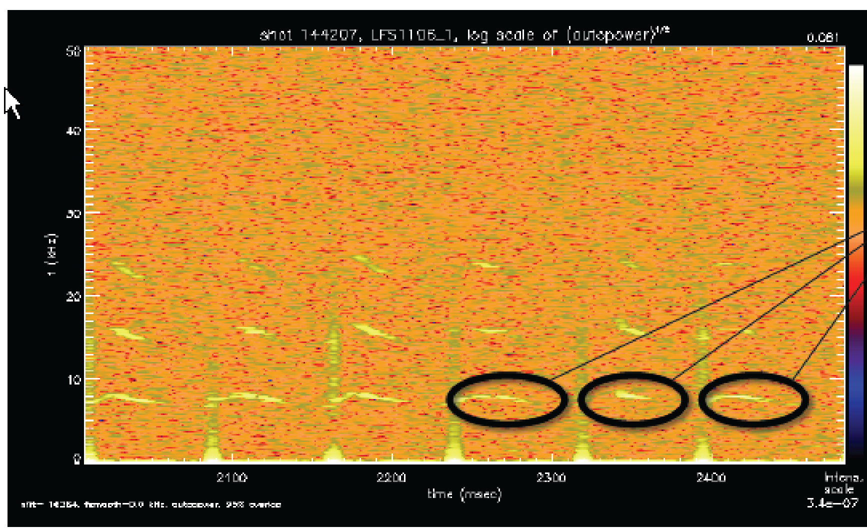

Early "post-cursor" type mode. Many features qualitatively similar to the downshifted mode observed in the oval case.

Bean (shots 144207, 08, 10)

Initial nonlinear studies showed dramatic difference between the bean and the oval shaped discharge with the exact same transport parameters!

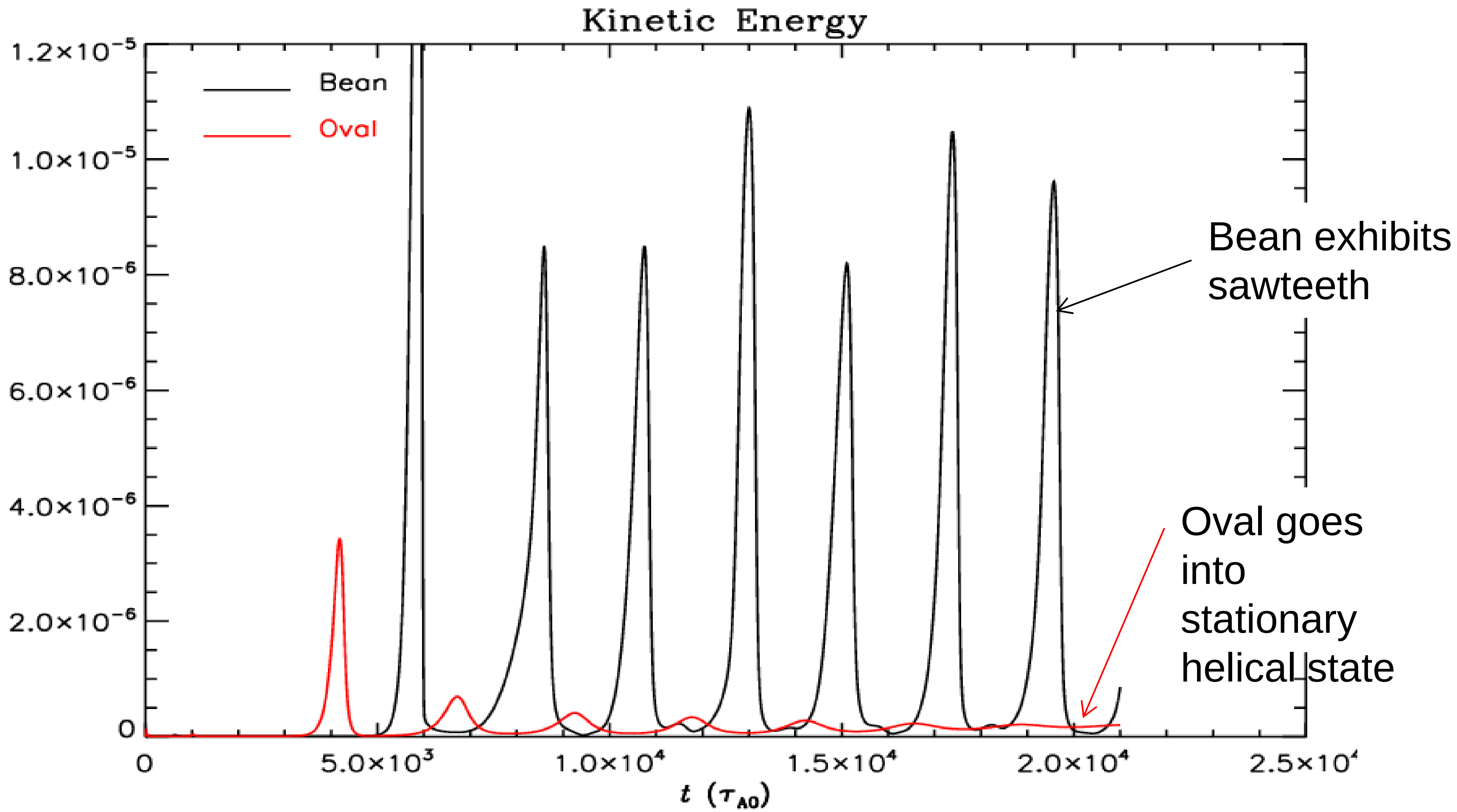

Stationary Pressure for DIII-D Oval (shot 118164)

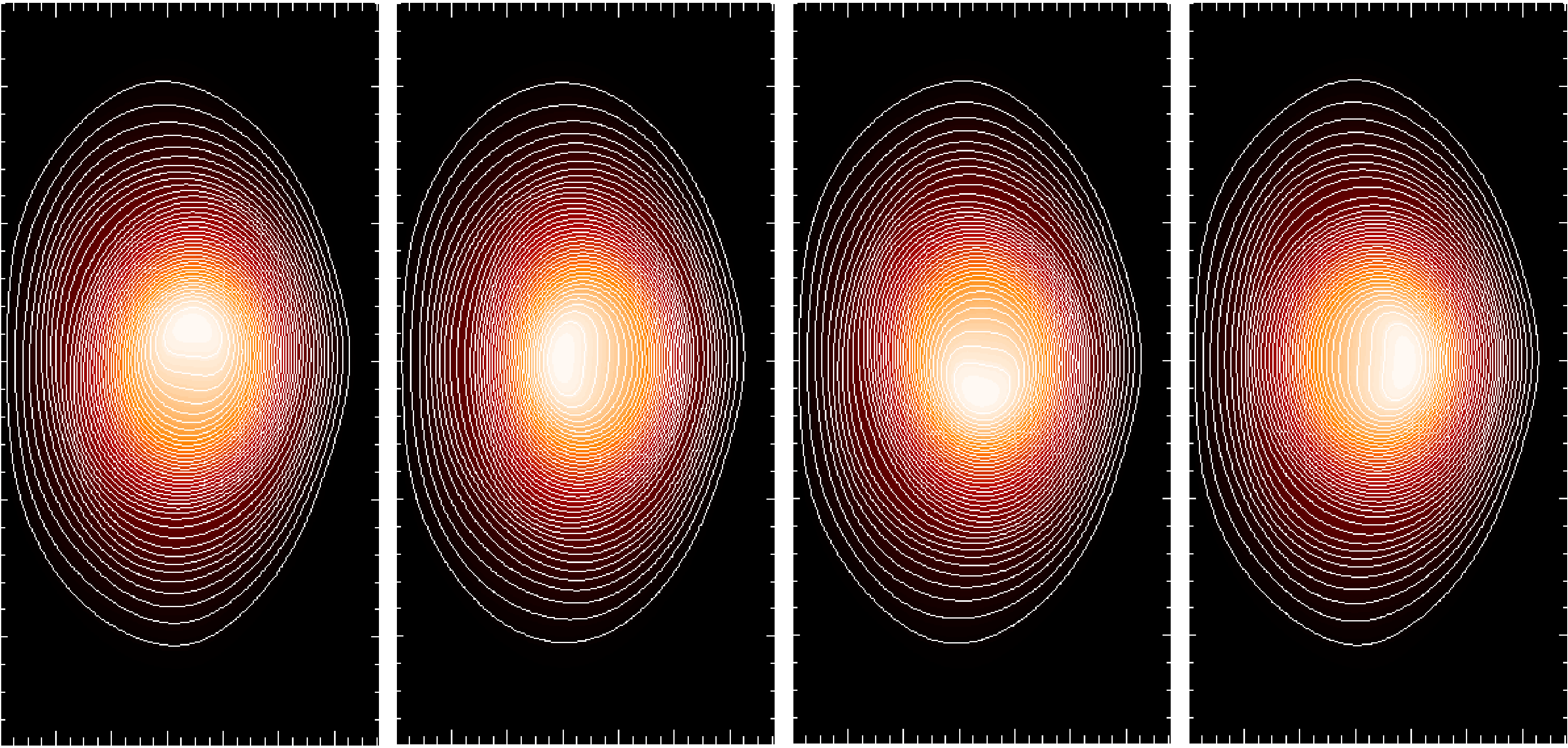

φ = 0°   φ = 90°   φ = 180°   φ = 270°

Stationary Current Density for DIII-D Oval (shot 118164)

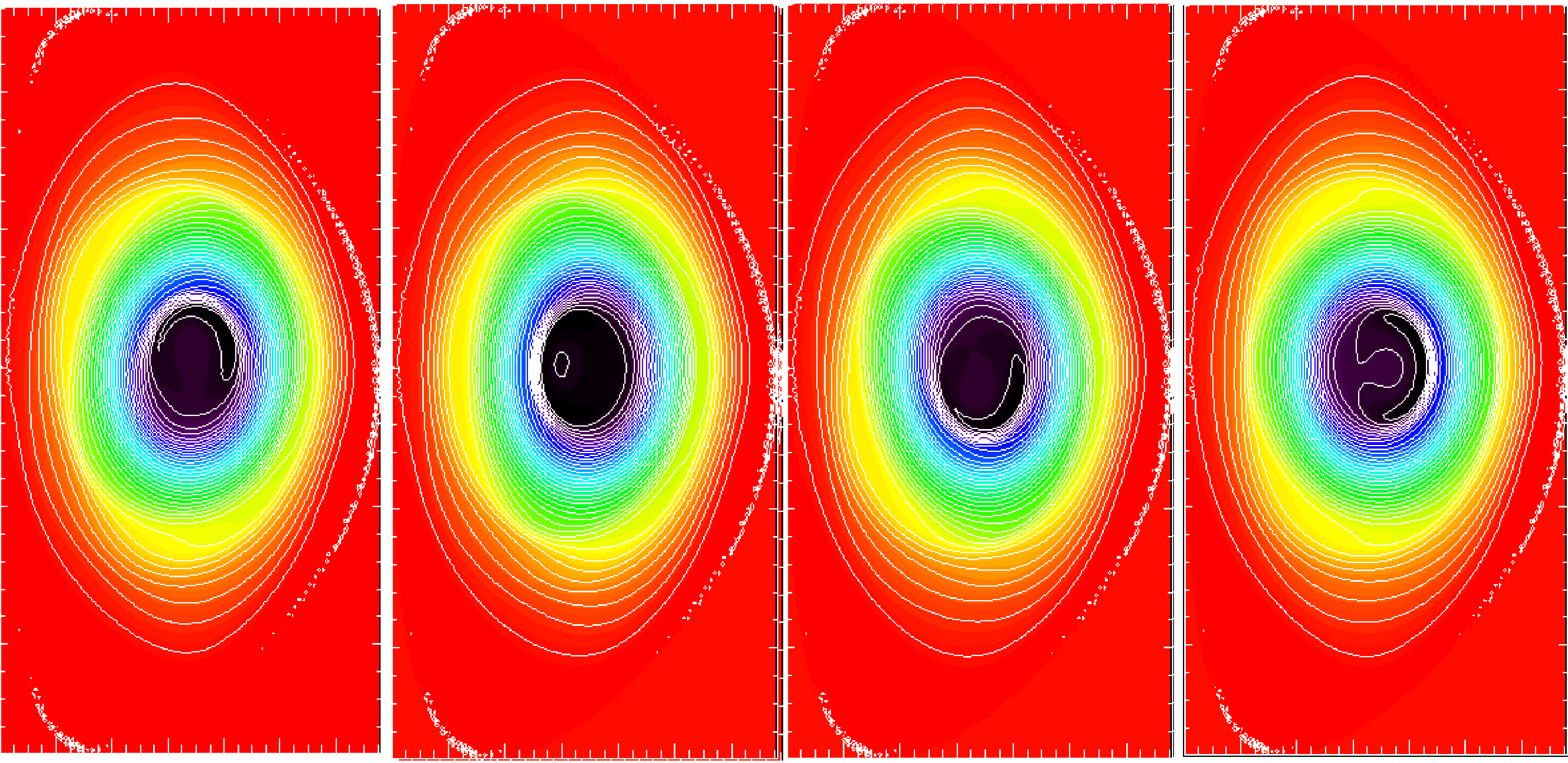

$\varphi = 0^o$ $\varphi = 90^o$ $\varphi = 180^o$ $\varphi = 270^o$

Stationary velocity stream function for DIII-D Oval (shot 118164)

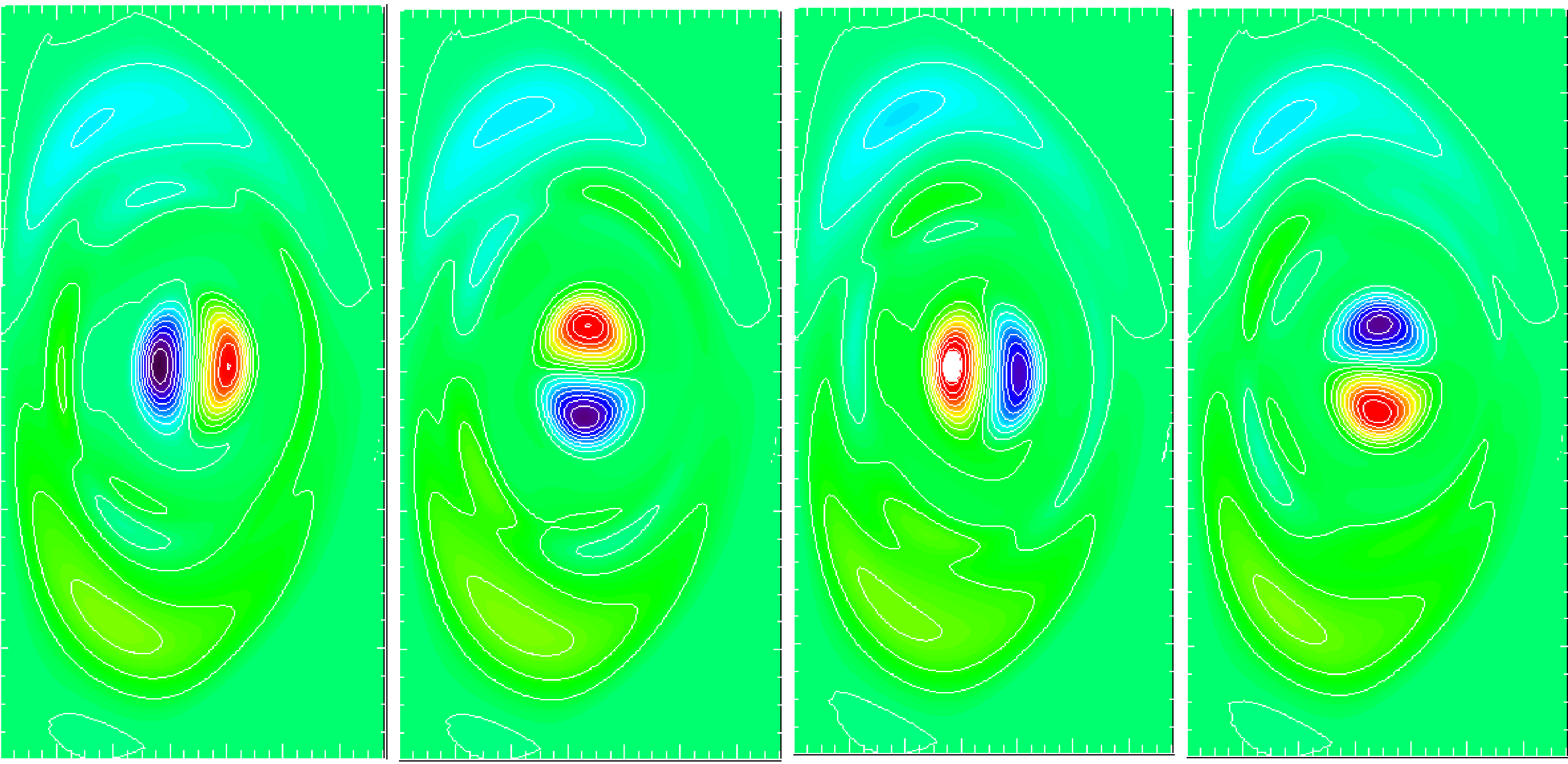

$\varphi = 0^o$ $\varphi = 90^o$ $\varphi = 180^o$ $\varphi = 270^o$

Oval stationary state has many islands

$q_{min} = 1.01$

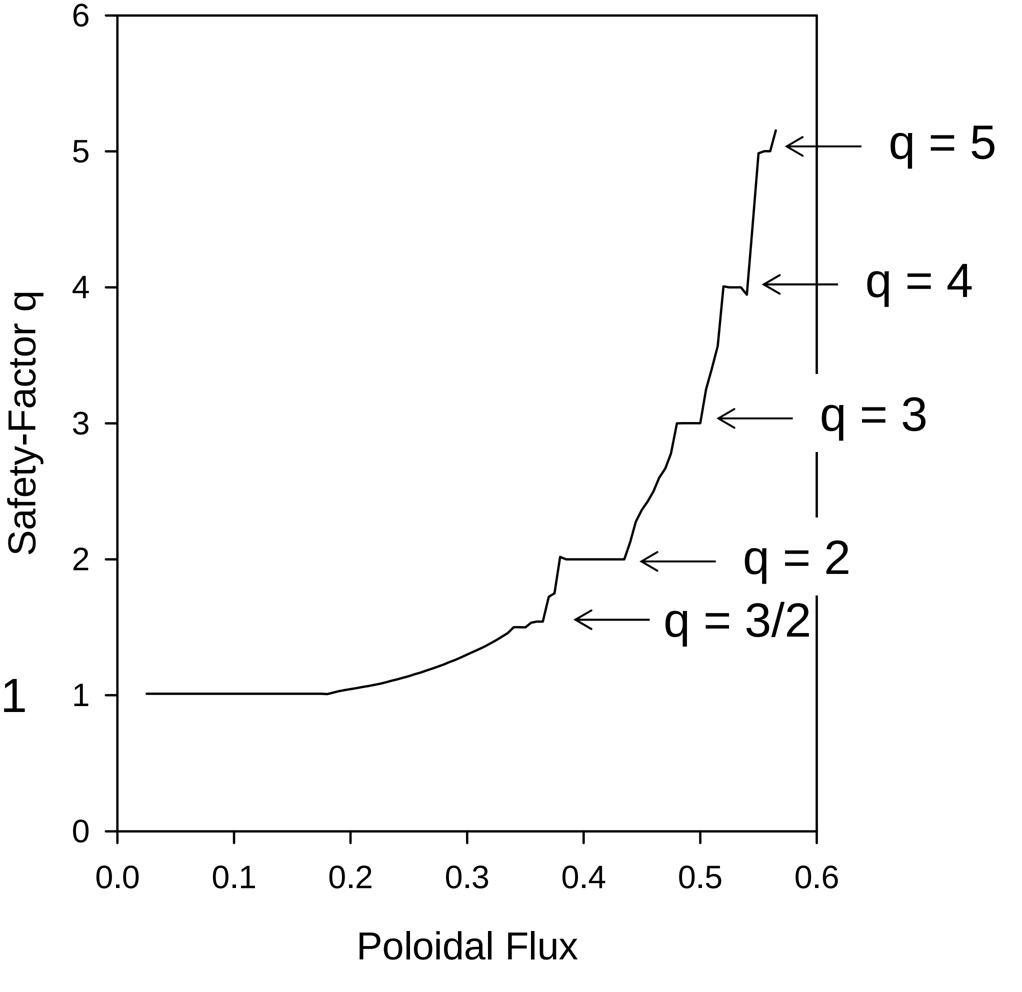

Original run repeated with new code with temperature advance rather than pressure.

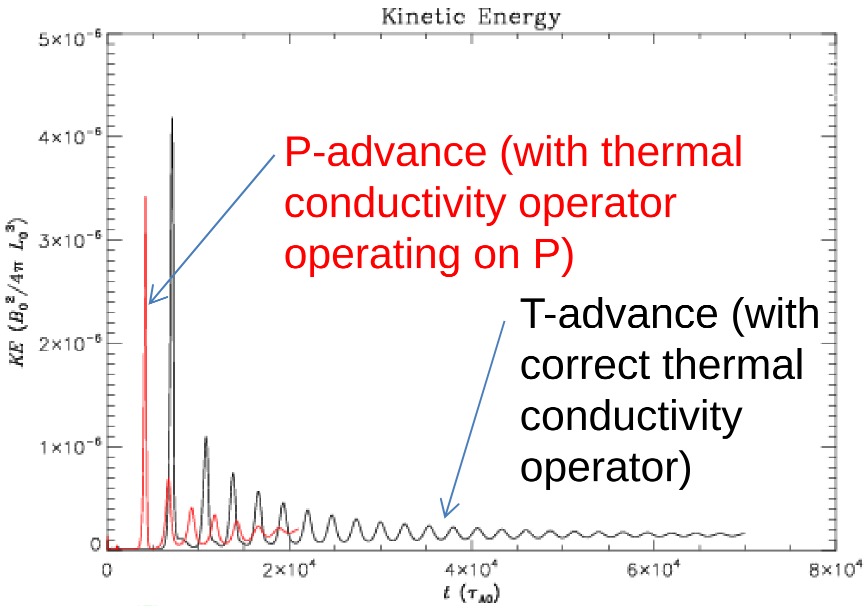

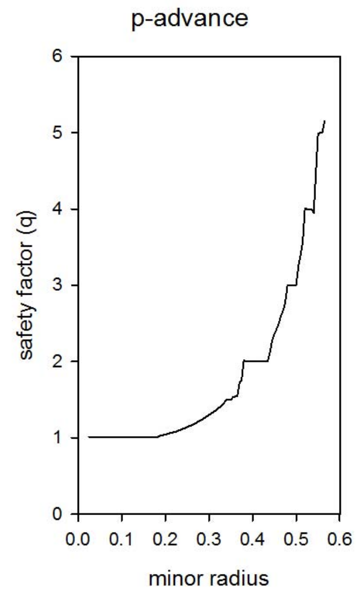

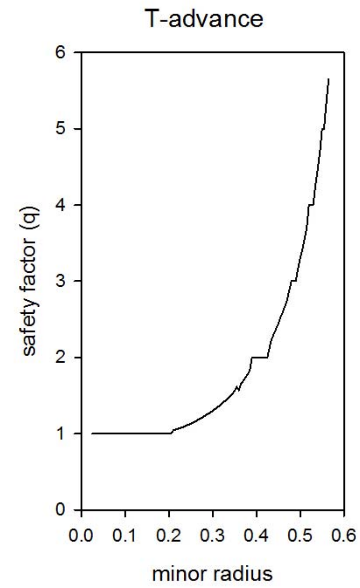

P-advance

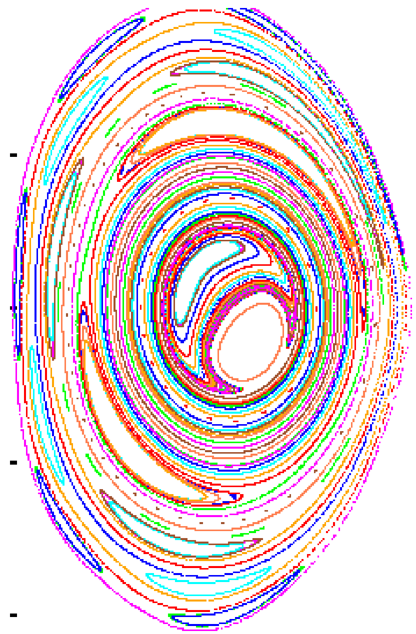

T-advance

- T-advance (more realistic) took longer to settle into a stationary state
- q-profiles and Poincare plots are similar…many islands

Cuts across midplane show that old calculation (p-advance) had larger 3D pressure distortion that newer (T-advance)

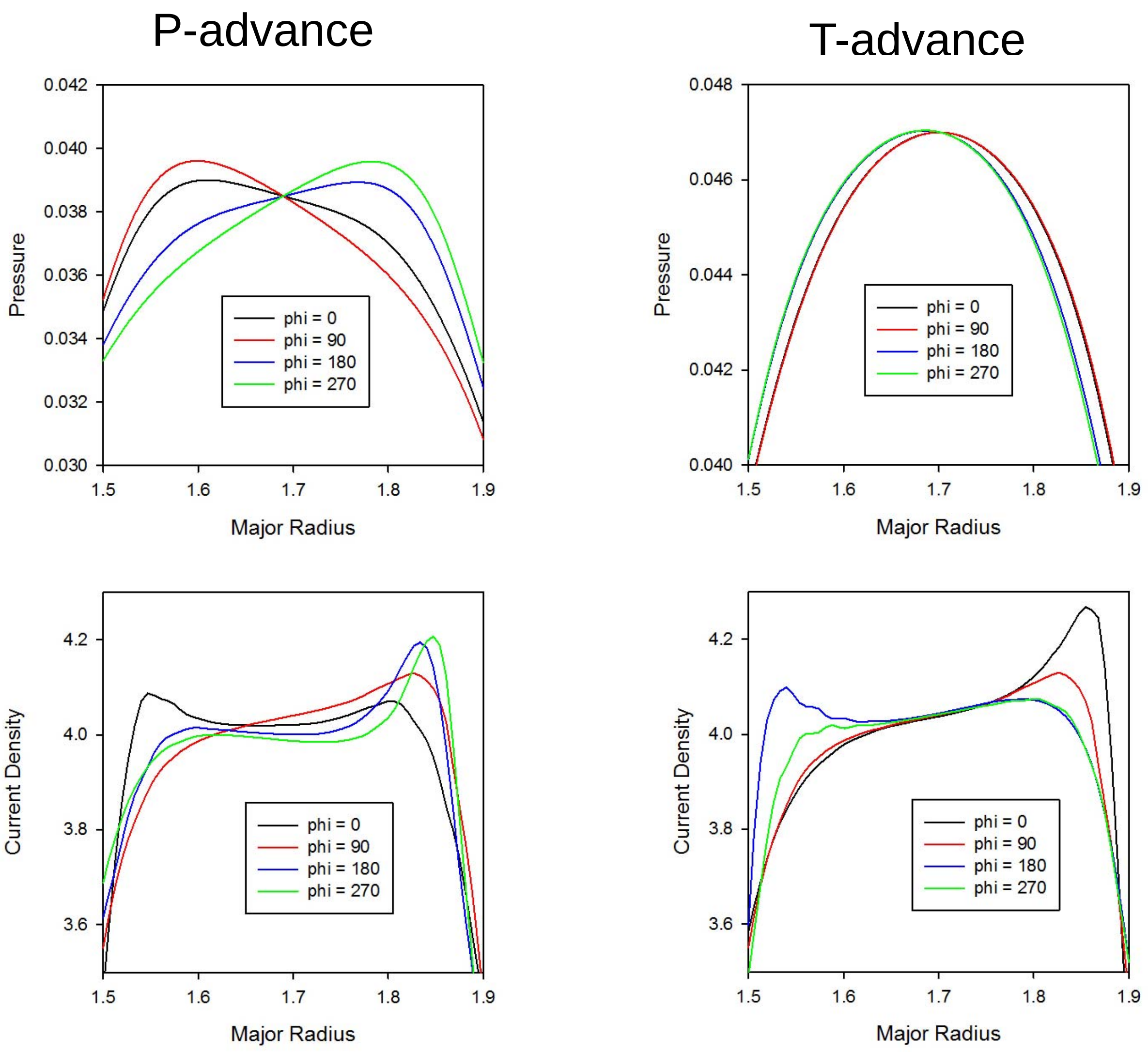

Doubling the toroidal resolution shows markedly different behavior … periodic sawteeth

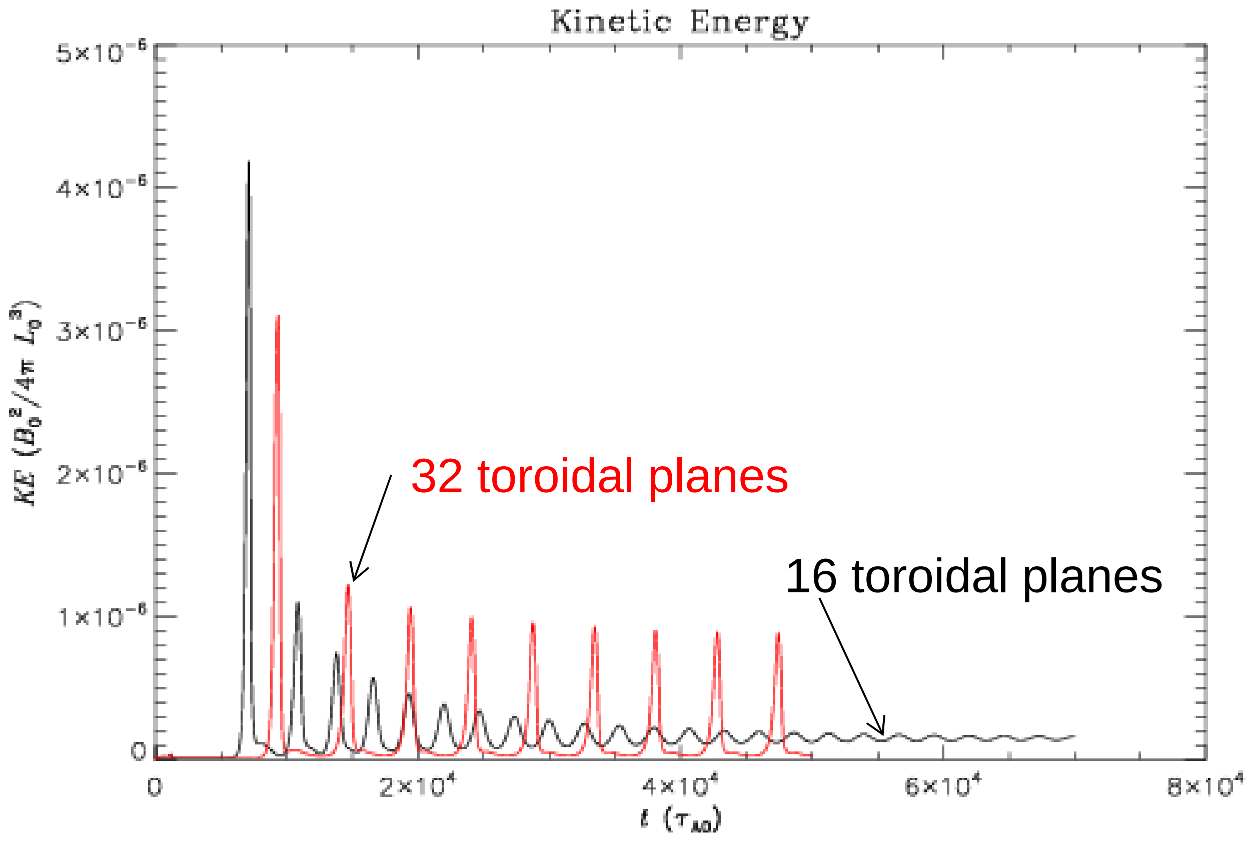

- In higher resolution case, plasma continues to exhibit sawteeth
- Is this due to a more accurate solution (low resolution case wrong?) or evidence of a bifurcation?

Toroidal cuts of electron temperature during a single sawtooth cycle. Note that crash occurs between time points 3 and 4.

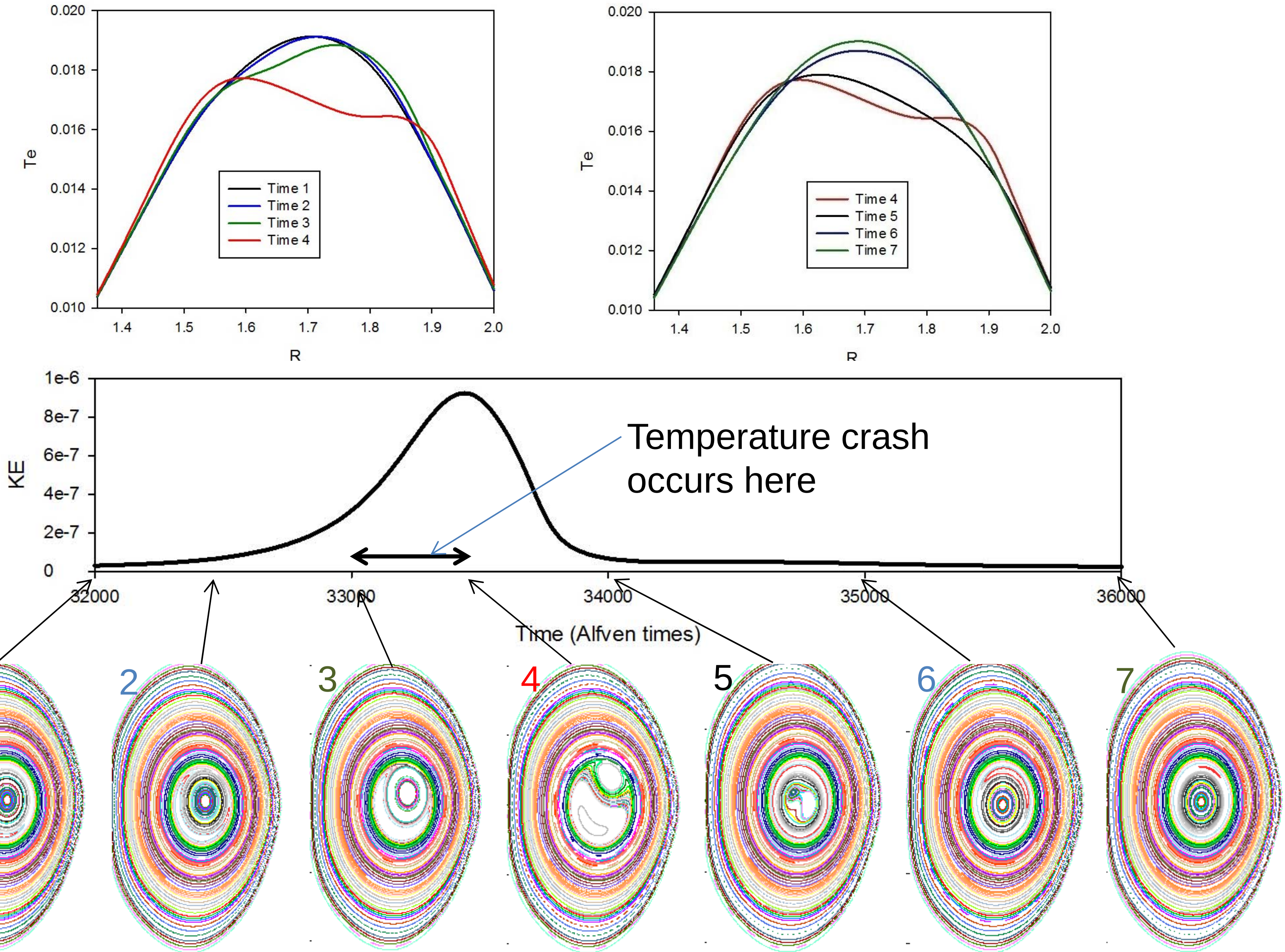

Toroidal cuts of electron density during a single sawtooth cycle.
(Note it increases where plasma temperature decreases)

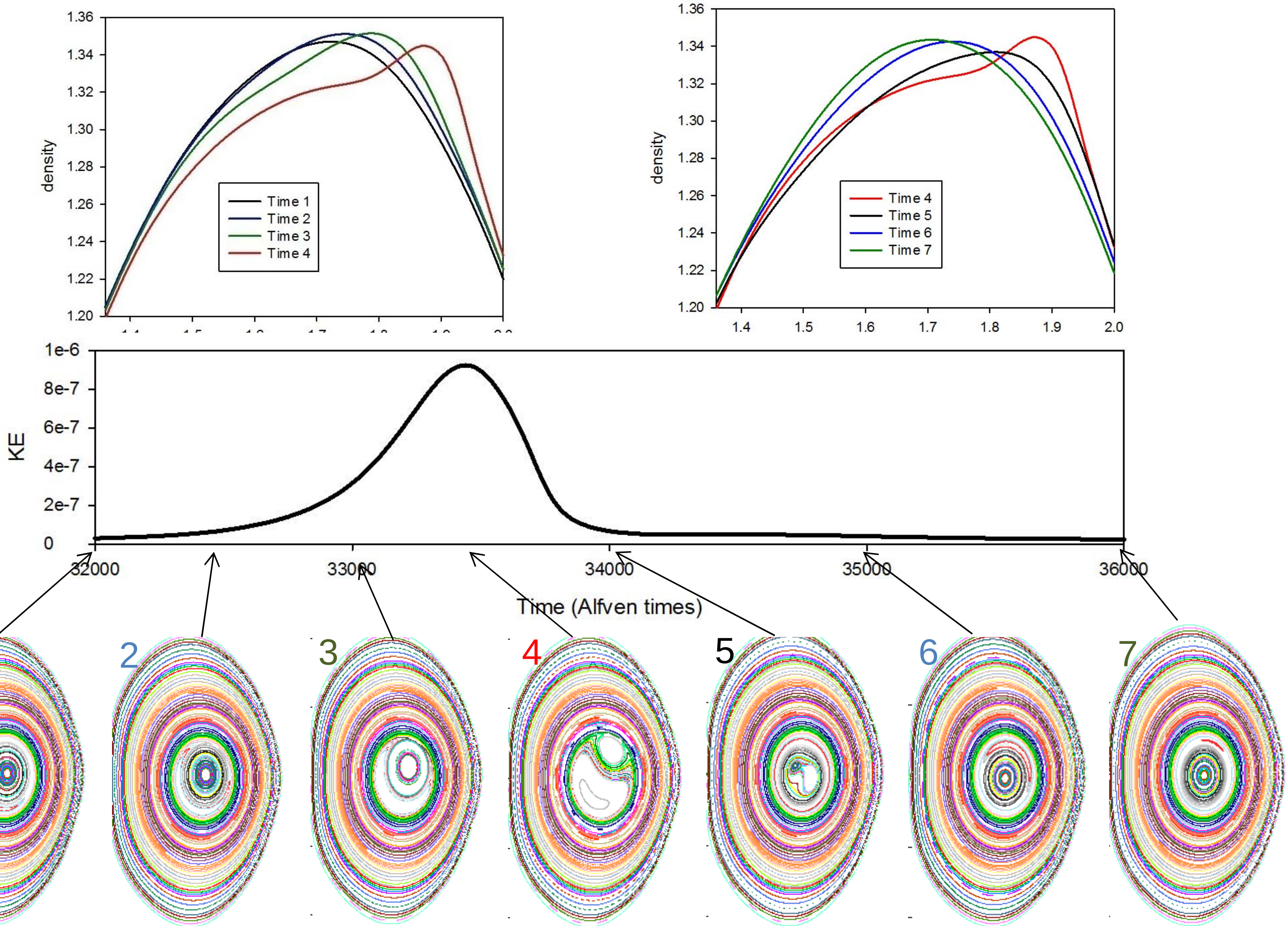

Toroidal cuts of current density during a single sawtooth cycle. At time 4, when current sheet is maximum, temperature has already crashed.

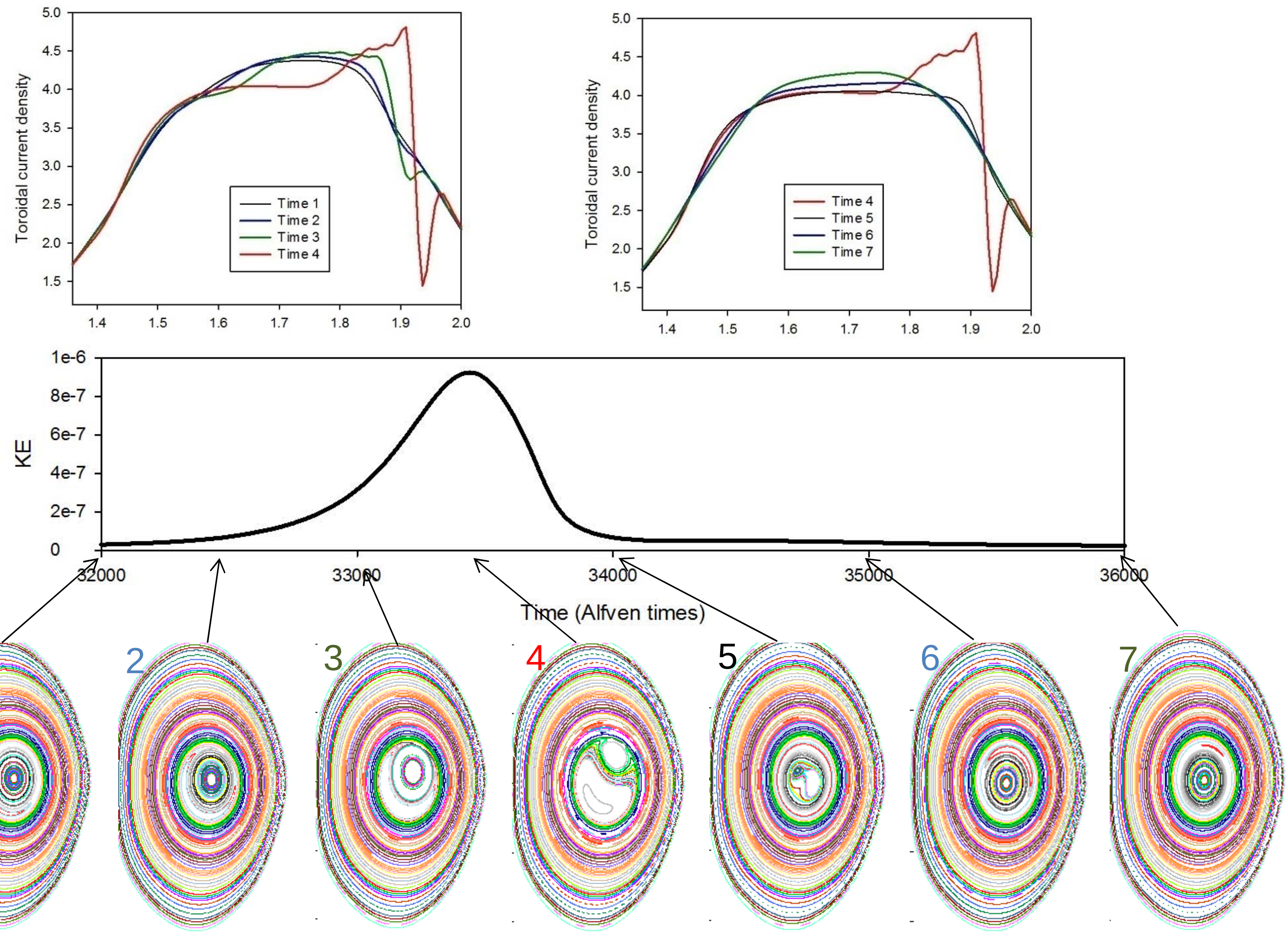

Evolution of safety factor during a single sawtooth cycle.

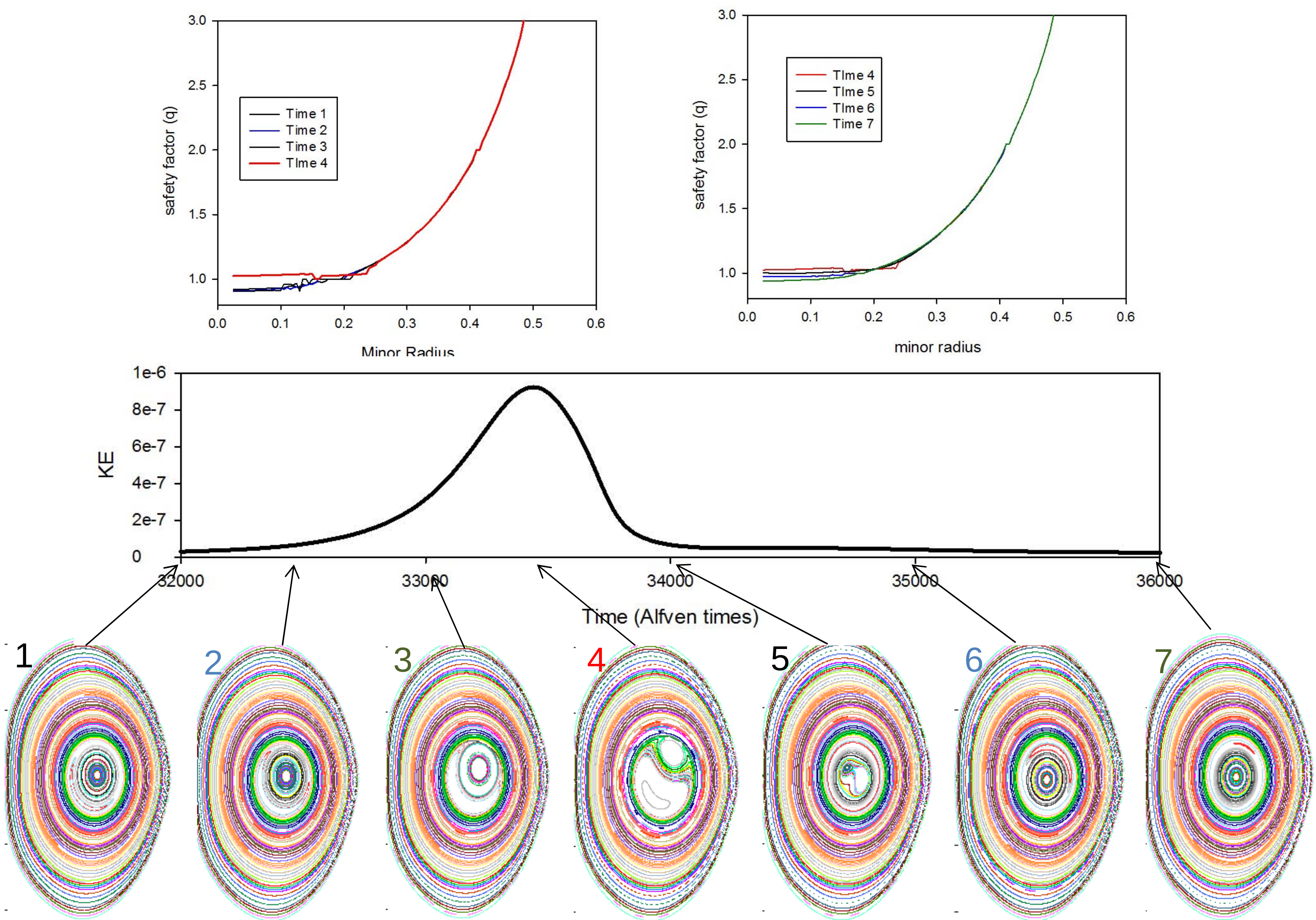

Summary of 16 plane vs 32 plane

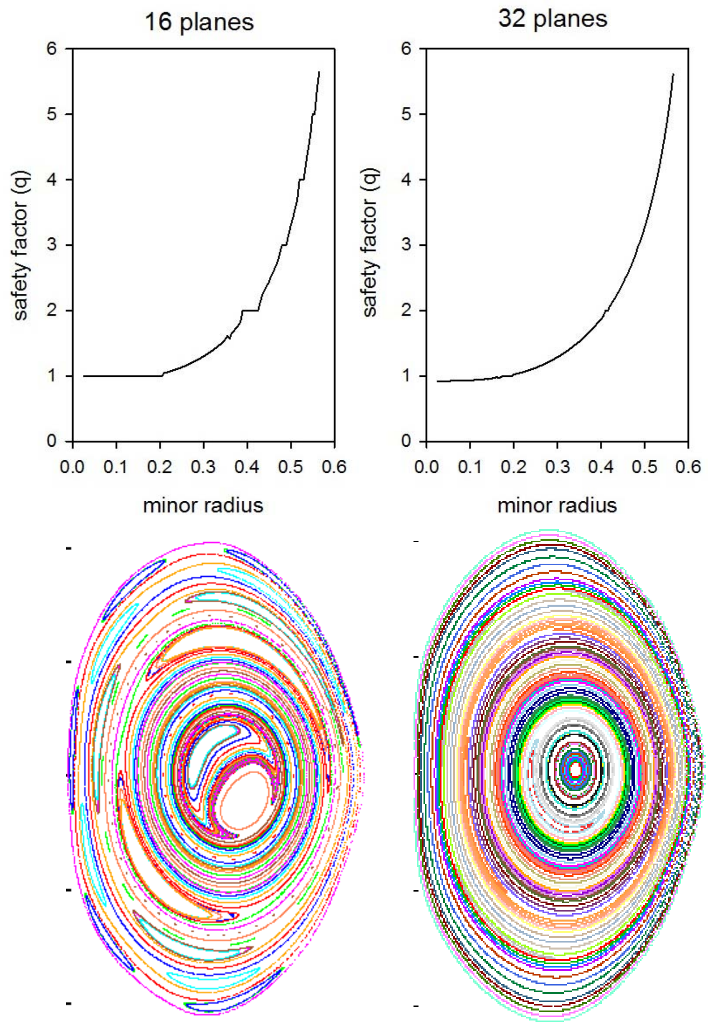

- 16 plane case goes into stationary state with many islands
- 32 plane case exhibits sawtoothing. Good surfaces exist between sawteeth.

Questions:

1. Why are 16 plane case and 32 plane case so different? Initialization, accuracy, or something else?
2. Now running 64 plane case

2-fluid split algorithm

Recall the split algorithm consists of a velocity solve followed by separate solves for the fields, the temperatures, and the density.

$$\begin{bmatrix} U \\ \omega \\ \chi \end{bmatrix}^{n+1} \rightarrow \begin{bmatrix} \psi \\ F \end{bmatrix}^{n+1} + \begin{bmatrix} T_e \\ T_i \end{bmatrix}^{n+1} + \left[n \right]^{n+1}$$

1. How is the velocity solve modified by 2F terms ?
2. How is the magnetic field solve modified by 2F terms?

$$\mathbf{V} = R^2 \nabla U \times \nabla \varphi + \boldsymbol{\omega} R^2 \nabla \varphi + R^{-2} \nabla_\perp \chi$$

$$\mathbf{B} = \nabla \psi \times \nabla \varphi - \nabla_\perp f' + F \nabla \varphi : \qquad \nabla_\perp^2 f = F - F_0$$

$$p_e = n T_e \quad \& \quad p_i = n T_i$$

modified 2-fluid algorithm for velocity solve

$$nM_i\dot{\mathbf{V}} = \left(\mathbf{J} + \theta\delta t\dot{\mathbf{J}}\right)\times\left(\mathbf{B} + \theta\delta t\dot{\mathbf{B}}\right) - \nabla\left(p + \theta\delta t\dot{p}\right) + \cdots$$

$$\dot{\mathbf{B}} = \nabla\times\left[\left(\mathbf{V} + \theta\delta t\dot{\mathbf{V}}\right)\times\mathbf{B} \underbrace{-\frac{1}{ne}\left[\mathbf{J}\times\mathbf{B} - \nabla p_e - \nabla\bullet\Pi_e\right]}_{-\frac{M_i}{e}\left(\frac{\partial\mathbf{V}}{\partial t} + \mathbf{V}\bullet\nabla\mathbf{V}\right) - \frac{1}{ne}\left[\nabla p_i + \nabla\bullet\Pi_i\right]} + \cdots\right]$$

–Ion velocity form for 2F differential approximation operator

2F Implicit velocity advance becomes:

$$\left(nM_i - \theta^2\delta t^2 L_0 + \theta\delta t d_i L_1\right)\mathbf{V}^{n+1} = \left(nM_i + \theta\left(\theta - 1\right)\delta t^2 L_0 + \theta\delta t d_i L_1\right)\mathbf{V}^n + \cdots$$

Here, the two operators are defined as:

$$L_0\left\{\mathbf{V}\right\} = \left\{\nabla\times\left[\nabla\times\left(\mathbf{V}\times\mathbf{B}\right)\right]\right\}\times\mathbf{B} + \left(\nabla\times\mathbf{B}\right)\times\left[\nabla\times\left(\mathbf{V}\times\mathbf{B}\right)\right] + \nabla\left(\mathbf{V}\bullet\nabla p + \gamma p\nabla\bullet\mathbf{V}\right)$$

$$L_1\left\{\mathbf{V}\right\} = \left\{\nabla\times\left[\nabla\times\mathbf{V}\right]\right\}\times\mathbf{B} + \left(\nabla\times\mathbf{B}\right)\times\left[\nabla\times\mathbf{V}\right]$$

Verification on 2D GEM test problem

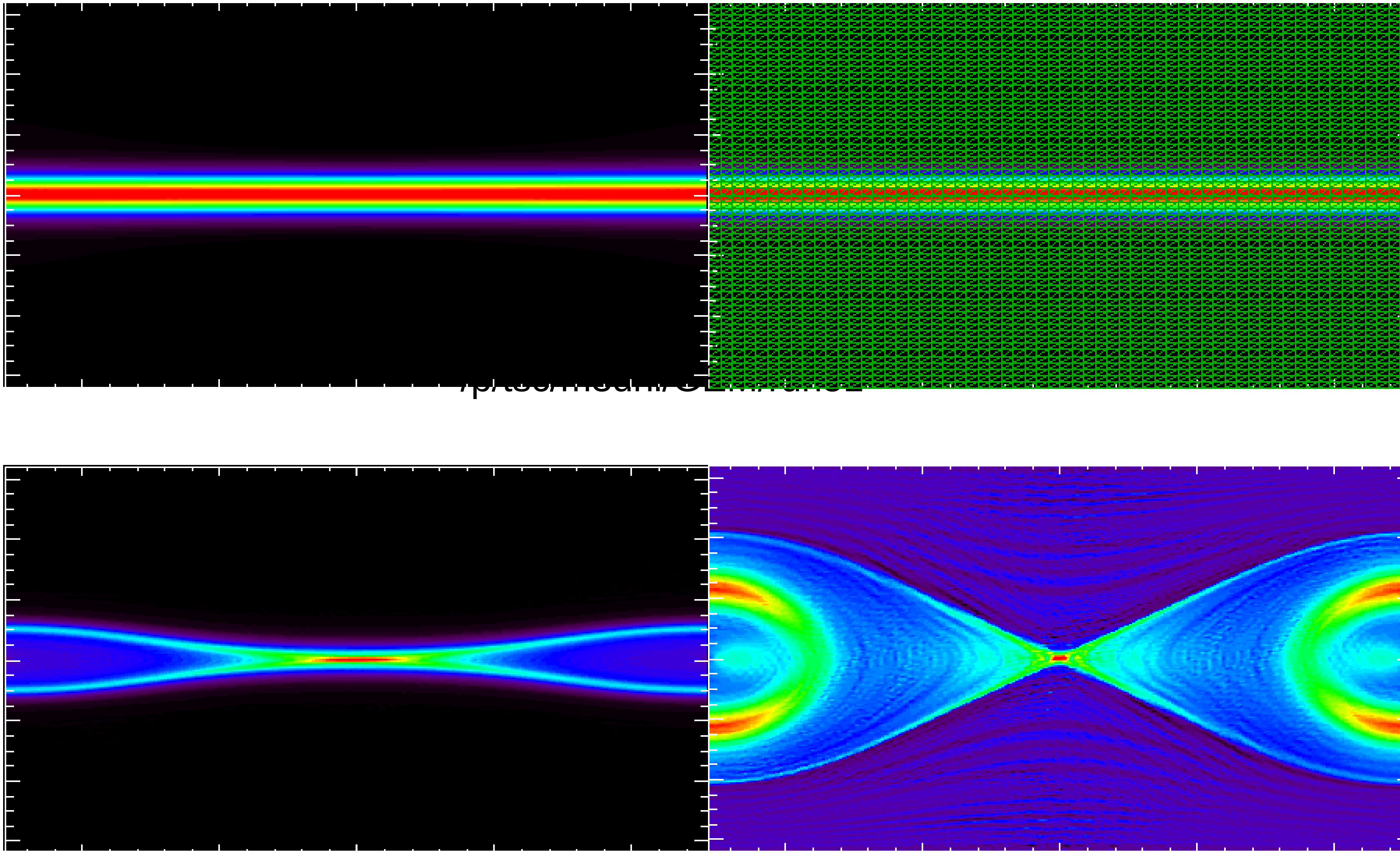

2F GEM timestep convergence study with (YES-dashed curves) and without (NO-solid curves) new operator in velocity equation

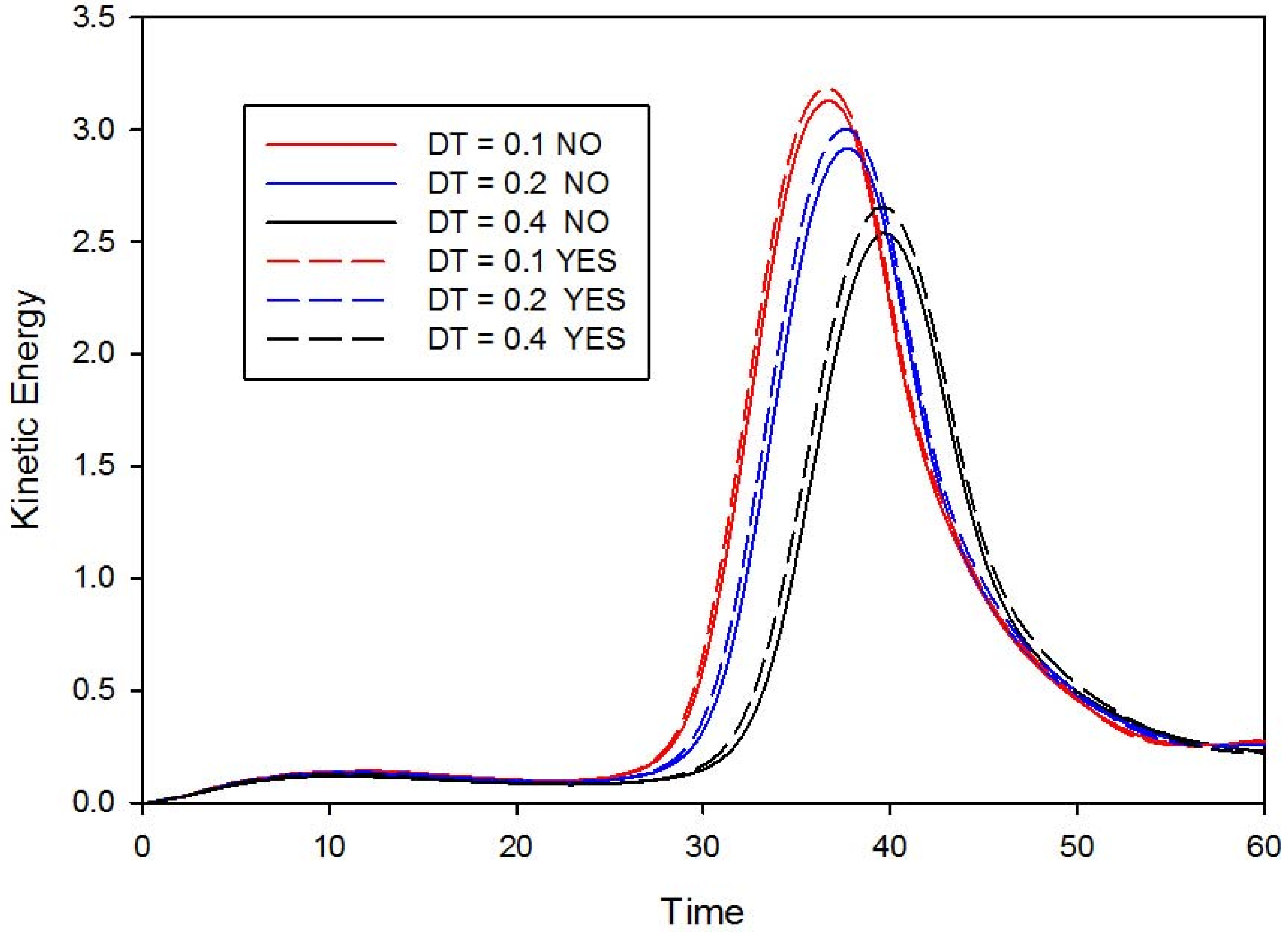

New terms appear to (slightly) improve time convergence!

An aside on the poloidal flux advance

jadv=0

$$\dot{\psi} = r^2[U,\psi] - r^2(U,f') - r^{-2}(\chi,\psi) - R_0^2[\chi,f'] + \eta\left[\Delta^*\psi - \lambda_H\Delta^*(\Delta^*\psi)\right] + \frac{d_i}{\rho}\left[[\psi,F^*] + (F^*,f') + \frac{1}{R^2}(\psi,\psi') + [\psi',f'] + p_e'\right] - \Phi'$$

$$\nabla_\perp \bullet \frac{1}{R^2}\nabla\Phi = \nabla_\perp \cdot \left[-\frac{F}{R_0^2R^2}\nabla_\perp U + \frac{\omega}{R^2}\nabla_\perp\psi + \omega\nabla_\perp f'\times\nabla\varphi + \frac{F}{r^2R^2}\nabla_\perp\chi\times\nabla\varphi\right]$$
$$+\nabla_\perp\cdot\eta\left[-\frac{1}{R^2}\nabla F\times\nabla\varphi - \frac{1}{R^2}\nabla f''\times\nabla\varphi + \lambda_H\nabla\left(\frac{1}{R^2}\nabla^2F + \frac{1}{R^4}F''\right)\times\nabla\varphi - \frac{1}{R^4}\nabla_\perp\psi' + \frac{1}{R^2}\lambda_H\nabla_\perp\left(\frac{1}{R^2}\Delta^*\psi'\right)\right]$$
$$+\nabla_\perp\cdot d_i\left[\frac{1}{R^4\rho}\Delta^*\psi\nabla_\perp\psi + \frac{F}{R^4\rho}\nabla_\perp F + \frac{F}{R^4\rho}\nabla_\perp f'' + \frac{1}{R^2\rho}\nabla_\perp p_e - \frac{F}{R^4\rho}\nabla_\perp\psi'\times\nabla\varphi + \frac{1}{R^2\rho}\Delta^*\psi\nabla_\perp f'\times\nabla\varphi\right]$$

jadv=1

$$\nabla_\perp\bullet\frac{1}{R^2}\nabla\dot{\psi} = \nabla_\perp\bullet\frac{1}{R^2}\nabla r^2[U,\psi] - \nabla_\perp\bullet\frac{1}{R^2}\nabla r^2(U,f') + \nabla_\perp\cdot\left[\frac{F}{R^2}\nabla_\perp U\right]' - \nabla_\perp\cdot\left[\frac{\omega}{R^2}\nabla_\perp\psi + \omega\nabla_\perp f'\times\nabla\varphi\right]'$$
$$-\nabla_\perp\bullet\frac{1}{R^2}\nabla r^{-2}(\chi,\psi) - \nabla_\perp\bullet\frac{1}{R^2}\nabla R_0^2[\chi,f'] - \nabla_\perp\cdot\left[\frac{F}{r^2R^2}\nabla_\perp\chi\times\nabla\varphi\right]' + \nabla_\perp\bullet\frac{1}{R^2}\nabla\eta\Delta^*\psi$$
$$+\nabla_\perp\cdot\left[\frac{\eta}{R^2}\nabla F^*\times\nabla\varphi + \frac{\eta}{R^4}\nabla_\perp\psi'\right]' + \nabla_\perp\bullet\frac{1}{R^2}\nabla\frac{d_i}{\rho}\left[[\psi,F^*] + (F^*,f') + \frac{1}{R^2}(\psi,\psi') + [\psi',f'] + p_e'\right]$$
$$-\nabla_\perp\cdot d_i\left[\frac{1}{R^4\rho}\Delta^*\psi\nabla_\perp\psi + \frac{F}{R^4\rho}\nabla_\perp F^* + \frac{1}{R^2\rho}\nabla_\perp p_e - \frac{F}{R^4\rho}\nabla_\perp\psi'\times\nabla\varphi + \frac{1}{R^2\rho}\Delta^*\psi\nabla_\perp f'\times\nabla\varphi\right]'$$

Original, published results on GEM problem used jadv=0 with hyper-resistivity. Now, we use jadv=1 with no hyper-resistivity (for η large enough)

Harned-Mikic terms

Dominant cross terms in field advance are marked in red

$$\frac{1}{R^2}\dot{F} = \nabla_\perp \bullet \left[-F\nabla_\perp U \times \nabla\varphi + \omega\nabla_\perp\psi \times \nabla\varphi - \frac{1}{R^4}F\nabla_\perp\chi - \omega\nabla_\perp f' \right]$$
$$+\nabla_\perp \bullet \eta \left[\frac{1}{R^2}\nabla F^* - \frac{1}{R^2}\nabla_\perp\psi' \times \nabla\varphi \right]$$
$$+d_i\nabla_\perp \bullet \left[\frac{1}{\rho R^2}\Delta^*\psi\nabla_\perp\psi \times \nabla\varphi + \frac{F}{\rho R^2}\nabla_\perp F^* \times \nabla\varphi + \frac{1}{\rho}\nabla_\perp p_e \times \nabla\varphi + \color{red}{\frac{F}{\rho R^4}\nabla_\perp\psi'} - \frac{1}{\rho R^2}\Delta^*\psi\nabla_\perp f' \right]$$

$$\nabla_\perp \bullet \frac{1}{R^2}\nabla\dot{\psi} = \nabla_\perp \bullet \frac{1}{R^2}\nabla r^2[U,\psi] - \nabla_\perp \bullet \frac{1}{R^2}\nabla r^2(U, f') + \nabla_\perp \cdot \left[\frac{F}{R^2}\nabla_\perp U \right]' - \nabla_\perp \cdot \left[\frac{\omega}{R^2}\nabla_\perp\psi + \omega\nabla_\perp f' \times \nabla\varphi \right]'$$
$$-\nabla_\perp \bullet \frac{1}{R^2}\nabla r^{-2}(\chi,\psi) - \nabla_\perp \bullet \frac{1}{R^2}\nabla R_0^2[\chi, f'] - \nabla_\perp \cdot \left[\frac{F}{r^2 R^2}\nabla_\perp\chi \times \nabla\varphi \right]'$$
$$+\nabla_\perp \bullet \frac{1}{R^2}\nabla\eta\Delta^*\psi + \nabla_\perp \cdot \left[\frac{\eta}{R^2}\nabla F^* \times \nabla\varphi + \frac{\eta}{R^4}\nabla_\perp\psi' \right]'$$
$$+\nabla_\perp \bullet \frac{1}{R^2}\nabla\frac{d_i}{\rho}\left[[\psi, F^*] + (F^*, f') + \frac{1}{R^2}(\psi,\psi') + [\psi', f'] + p_e' \right]$$
$$-\nabla_\perp \cdot d_i \begin{bmatrix} \frac{1}{R^4\rho}\Delta^*\psi\nabla_\perp\psi \color{red}{+ \frac{F}{R^4\rho}\nabla_\perp F^*} + \frac{1}{R^2\rho}\nabla_\perp p_e \\ -\frac{F}{R^4\rho}\nabla_\perp\psi' \times \nabla\varphi + \frac{1}{R^2\rho}\Delta^*\psi\nabla_\perp f' \times \nabla\varphi \end{bmatrix}'$$

$$(\ )' \equiv \frac{\partial}{\partial\varphi}(\ )$$

$$\mathbf{B} = \nabla\color{red}{\psi} \times \nabla\varphi - \nabla_\perp f' + \color{red}{F}\nabla\varphi : \qquad \nabla_\perp^2 f = F - F_0$$

Harned-Mikic terms-2

Implicit advance for the field variables have the Harned-Mikic terms added to make the matrix more diagonal and improve the 3D iterative solution when 2F terms are present.

$$\nabla_\perp \bullet \frac{1}{R^2}\nabla_\perp \dot{\psi} + \left(\theta\,\delta t\, d_i\right)^2 (H_m)\nabla_\perp \bullet \left[\underbrace{\frac{F}{R^4 n}\nabla_\perp \left(R^2 \nabla_\perp \bullet \frac{F}{R^4 n}\nabla_\perp \dot{\psi}''\right)}_{\left(\mathbf{B}\bullet\nabla\right)^2 \nabla_\perp^2}\right] = \cdots$$

$$\frac{1}{R^2}\dot{F} + \left(\theta\,\delta t\, d_i\right)^2 (H_m)\underbrace{\frac{F}{nR^2}\nabla_\perp \bullet \frac{F}{nR^4}\nabla_\perp \dot{F}''}_{\left(\mathbf{B}\bullet\nabla\right)^2 \nabla_\perp^2} = \cdots$$

Eigenvalues of the field matrix after preconditioning (with no HM terms)

$d_i = 0$ | $d_i = .045$ | $d_i = .090$

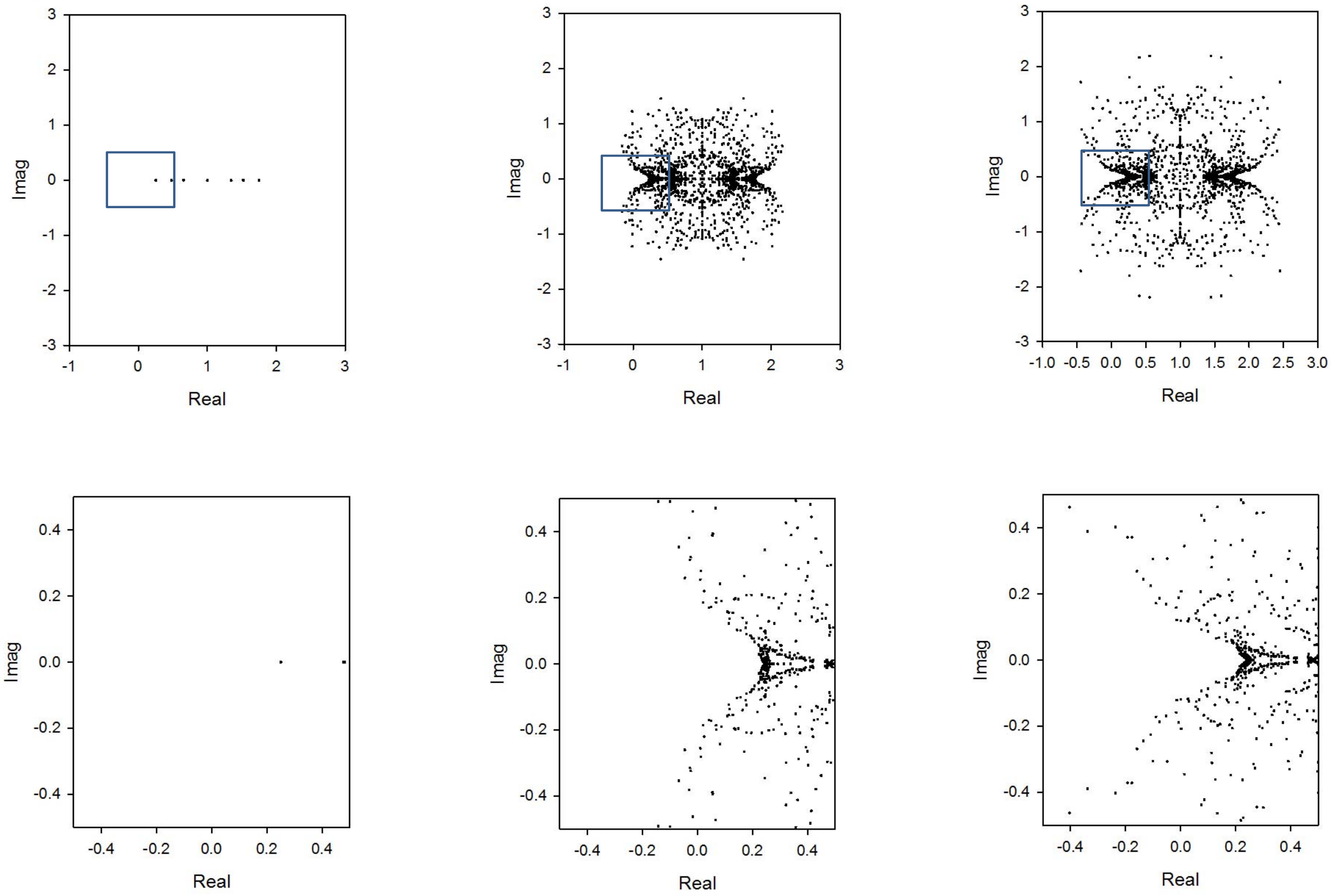

Eigenvalues of the field matrix with d_i=.09 after preconditioning showing the effect of the Harned-Mikic terms.

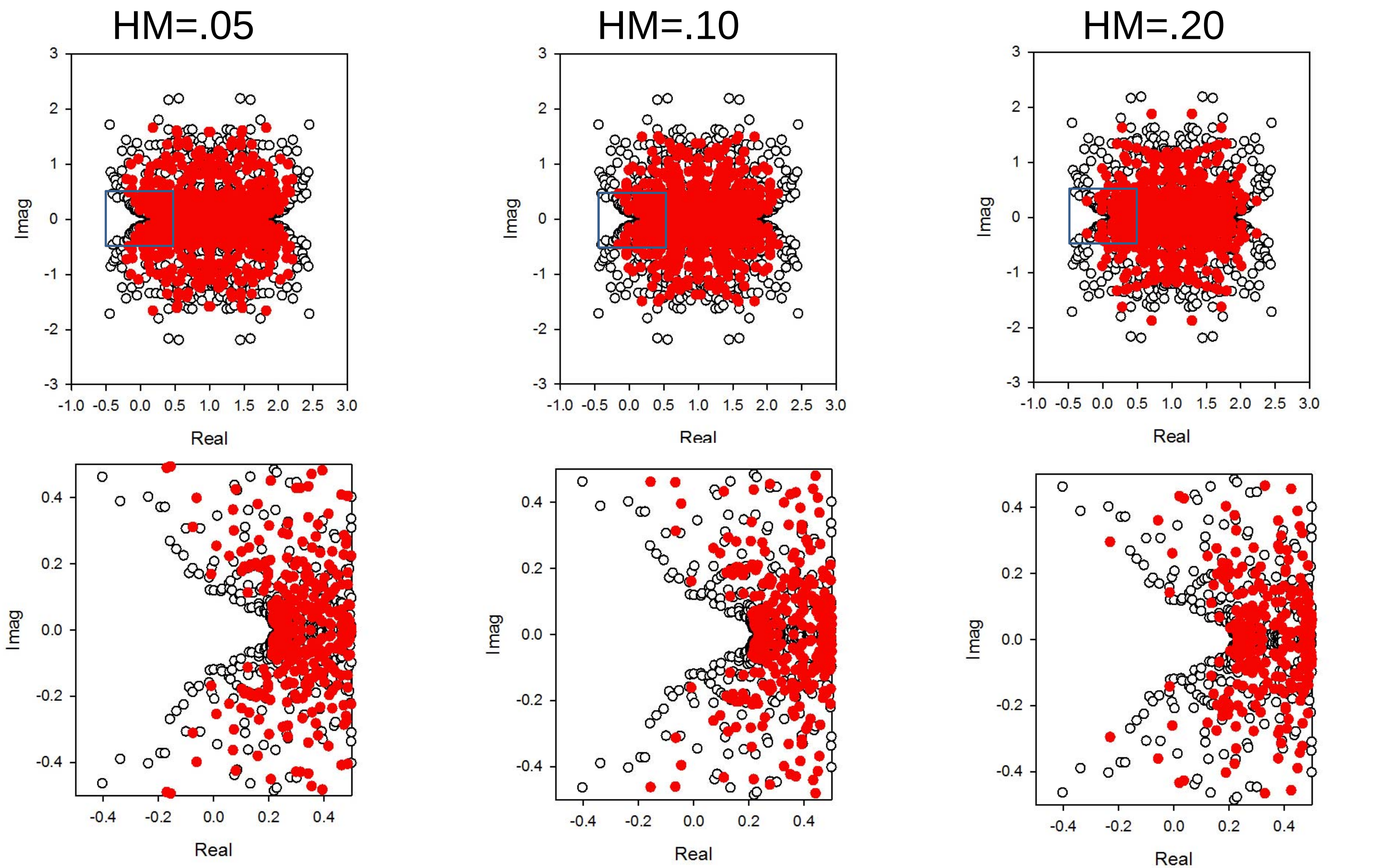

There is some improvement in the ratio of largest to smallest eigenvalues, but since matrix is non-symmetric, the significance of this is unclear.

Summary

- Preconditioner effect on eigenvalues
  - Block Jacobi preconditioner very effective in improving condition number of 3D matrix in velocity solve.
- New time advance options
  - Now advance the temperatures rather than the pressures
- Resistive MHD long-time runs with density and 2 temperatures
  - stationary helical states with many magnetic islands
  - sawtoothing discharges show rapid temperature collapse
  - Bifurcation or non-convergence ???
- 2-fluid algorithm
  - Ion velocity form for velocity preconditioner
    - Appears to improve time convergence in 2D test problem
  - Harned-Mikic terms
    - Needed for convergence of field solve iteration in 3D but not fully understood in terms of the eigenvalues
    - Testing in 3D underway